The Multiple Periodic Structure Antenna Design

Z. L. Ma, L. J. Jiang, S. Gupta, and W. E. I. Sha
Department of Electrical and Electronic Engineering, The University of Hong Kong, Hong Kong, China

Abstract— In this paper, the generalized analysis and novel application of the multiple periodic (MP) structure are proposed. Both transmission and radiation performances of one dimensional MP structures are studied. The dispersion relations are analyzed from both layered media (distributive) and lumped circuits aspects. Regarding each aspect, both non-dispersive (conventional) and dispersive (composite right/left-handed (CRLH)) materials are discussed. It is found that with the increase of the periodicity, multiple stopbands are open up due to the reflections. Meanwhile the space harmonic modes' separation distance is reduced in the dispersion diagrams. It leads to simultaneously dualistic (right- and left-handed) radiation performance and multi-beam property, and more abundant radiation modes are excited at relatively lower frequencies comparing with conventional periodic structures. A general dispersion relation formula and a general Bragg condition for MP structures are derived. The dispersion relation is simply described by the former, and the latter helps to indicate the stopbands locations and engineer the dispersion relation consequently. Applications of MP structures to phase reversal (PR) antennas are also presented in this paper. They experimentally verifies both transmission and radiation characteristics of MP structures. In each analysis, single (SP), double (DP) and triple periodic (TP) structures are presented and compared. This work would also contribute to designs of multi-band devices.

1. INTRODUCTION

In past decades, periodic structures were widely applied in both optics and microwave areas. In optics, the characteristics of dielectric layered media are studied [1]. While, in microwave fields, a large number of studies are conducted on both dispersive (composite right/left-handed (CRLH)) and non-dispersive (conventional) materials. Their leaky-wave radiation properties are also investigated [2–4]. However, most research works are focused on the conventional single periodic structures.

In this paper, we generalize the multiple periodically (MP) loaded structure analysis. Unified characterization of both transmission and radiation performances for both non-dispersive (conventional) and dispersive (CRLH) MP structures are presented. This work aims to explore the general property variations due to increasing periodicities that could be arbitrary (multiple). MP phase reversal (PR) antennas are presented in this paper as one application of the proposed concept. The transmission and radiation properties are examined. It is found that MP PR antennas support simultaneous forward and backward radiations and multiple radiation beams. We know that the indoor wireless link has some intrinsic effects would affect the link quality, such as multipath and mutual interference effect. One effective solution from physical layer perspective for it is to adopt multi-beam directional antenna. Therefore, the MP PR antenna can be a candidate for indoor wireless system or other multi-beam required applications. On the other hand, this work reveals the increasing number of stopbands and passbands. Therefore it also gives a strong support for various multi-band component designs.

2. THEORY

Figure 1(a) is an illustration of a typical MP structure, where each supercell consists of several different unit cells (UCs). The supercell periodically repeats along one dimension. All UCs and supercells are connected in series. The physical length of each UC is p.

2.1. Non-dispersive and Dispersive Media

For non-dispersive layered media, each UC has different refractive indices, $n_1, n_2, \ldots, n_m$. Based on the matrix theory, the transmission matrix can be written by the product of individual UCs' transmission matrices.

$$\begin{bmatrix} A & B \\ C & D \end{bmatrix} = \prod_{m=1}^{M} \begin{bmatrix} A_m & B_m \\ C_m & D_m \end{bmatrix} = \prod_{m=1}^{M} \frac{1}{2n_{m+1}} * \begin{bmatrix} (n_{m+1}+n_m)e^{-j\varphi_m} & (n_{m+1}-n_m)e^{j\varphi_m} \\ (n_{m+1}-n_m)e^{-j\varphi_m} & (n_{m+1}+n_m)e^{j\varphi_m} \end{bmatrix} \quad (1)$$

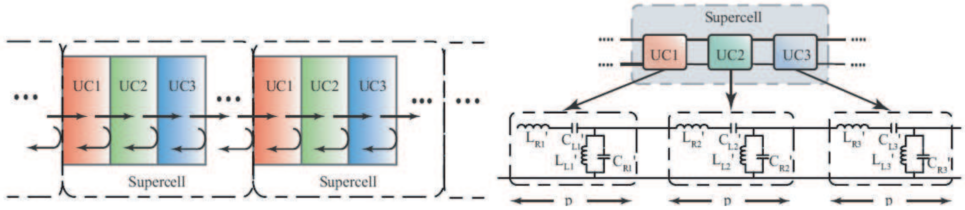

(a) (b)

Figure 1: (a) MP structure illustration and (b) equivalent circuit model for CRLH (dispersive) layered media.

where M is the total number of UCs in each supercell, and the phase change in one UC is $\varphi_m = n_m k_0 p$. m denotes UC index. k_0 is the wave vector of free space. According to the Bloch-Floquet theorem, we can obtain the dispersion relation

$$\cos\phi = \frac{A+D}{2} \tag{2}$$

where $\phi = \beta M p$ is the phase change in one supercell. β is the phase constant of the supercell. Using derivations shown above, we derive the dispersion relation for an arbitrary MP structure in a general format,

$$\cos\phi = \frac{1}{2^{(M+1)}\prod\limits_{i=1}^{M} n_i} \sum_{i=1}^{2^M} \left\{ \left(\prod_{j=1}^{M} S_i(j) \right) \left[\prod_{j=1}^{M} (n_j S_i(j) + n_{j+1} S_i(j+1)) \right] \cos(\bar{\varphi} \cdot \bar{S}_i) \right\} \tag{3}$$

where

$$\begin{cases} n_{j+1} = n_{j+1-M}, \quad if\ j+1 > M \\ \bar{S}_i^{\,1\times M} = [\pm1, \pm1, \pm1, \ldots, \pm1] \\ S_i(j+1) = S_i(j+1-M), \quad if\ j+1 > M \\ \bar{\varphi} = [\varphi_1, \varphi_2, \varphi_3, \ldots, \varphi_M] \end{cases} \tag{4}$$

$\bar{S}_i$ is a signs' vector with length of $1 \times M$. It has 2^M permutation types. For a given i, it stands for a kind of signs' permutation. According to the small reflection theorem, discontinuities on the MP structures cause multiple reflections and further lead to occurrence of stopbands. When reflected waves from UCs add in phase, the reflection will be the strongest, and the stopbands will be open up. As the Figure 1 shown, the round-trip phase in each UC is $2\varphi_1, 2\varphi_2, \ldots, 2\varphi_m$. The strongest reflection condition is

$$2\varphi_1 + 2\varphi_2 + 2\varphi_3 + 2\varphi_4 + \ldots. + 2\varphi_m = 2\pi q \tag{5}$$

where q is integer. Thus, we can obtain a general Bragg condition for MP structure,

$$\sum_{i=1}^{m} \varphi_i = q\pi \tag{6}$$

According to the derived general dispersion formula, the dispersion relations of SP, DP and TP non-dispersive media are presented in Figures 2(a)–(c). We can see that the SP structure does not have stopband in the given frequency range, and the DP and TP structures have one and two stopbands, respectively. We can easily find out the quantity relation between the periodicity M and the maximum number of stopbands N_s, $N_s = M - 1$. Besides, since we keep the UCs' lengthes same, the space harmonic modes' separation distance is correspondingly reduced. For SP, DP and TP structures, the separation distances are $2\pi/p$, $2\pi/2p = \pi/p$, $2\pi/3p$, respectively. In this figure, the general Bragg condition is also verified. The dash lines are $(\sum_{i=1}^{m} \varphi_i)/(mp)$. It is very obvious that the frequency points which satisfy general Bragg condition all fall into stopbands.

For the dispersive material, Figure 1(b) gives an illustration to the MP CRLH structure. The equivalent circuit model is shown. L'_R, C'_R, L'_L and C'_L are per-unit-length components. The refractive index of the CRLH structure can be represented by [4],

$$n(\omega) = c\left(\frac{1}{\omega'_R} - \frac{\omega'_L}{\omega^2}\right), \quad \text{and} \quad \omega'_L = \frac{1}{\sqrt{L'_L C'_L}}, \quad \omega'_R = \frac{1}{\sqrt{L'_R C'_R}} \tag{7}$$

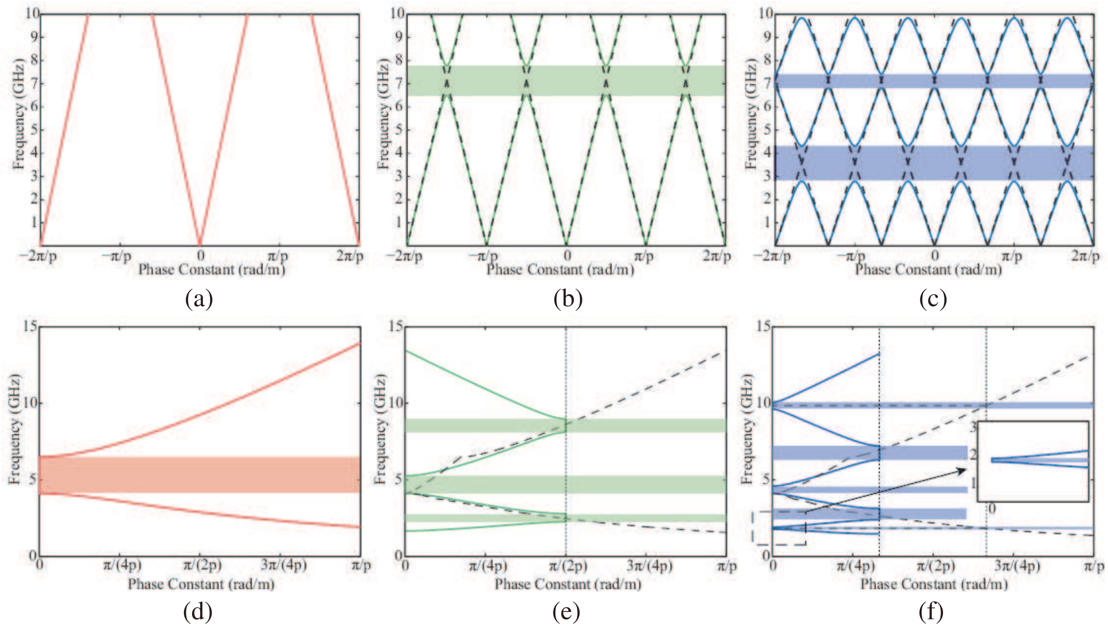

Figure 2: Dispersion Relations for (a)–(c) non-dispersive and (d)–(f) dispersive SP, DP and TP layered media. The solid lines are the dispersion curves. The dash lines stand for the general Bragg condition curves. The shadow regions refer to stopbands.

Here c is the light speed. w is the angular frequency. Substituting Equation (7) into (3), the dispersion relation for CRLH media can be obtained. Figures 2(d)–(f) present dispersion relations for SP, DP and TP CRLH structures. Similarly, the relation between the periodicity M and the maximum number of stopbands N_s can be summarized as $N_s = 2M - 1$. The space harmonic's period is also reduced correspondingly. The general Bragg condition is also verified in this figure. It shows that the general Bragg condition is also suitable for dispersive materials.

2.2. Non-dispersive and Dispersive Lumped Circuits

For the non-dispersive circuits, the transmission matrix can be represented as

$$\begin{bmatrix} A_m & B_m \\ C_m & D_m \end{bmatrix} = \begin{bmatrix} \cos\beta p j Z_{0m} & \sin\beta p \\ jY_{0m}\sin\beta p & \cos\beta p \end{bmatrix} \tag{8}$$

where Z_{0m} is the mth UC's characteristic impedance. Following the same derivation shown in Section 2.1, the dispersion relation can be obtained. Figures 3(a)–(c) show dispersion relations of SP, DP and TP transmission lines (TLs). The results are consistent with previous analysis. In this analysis, the frequency interval from 0 GHz to 8 GHz covers two harmonic frequency ranges. Hence, we see two and four stopbands for DP and TP cases, respectively. Within one harmonic frequency range (0 GHz to 4 GHz), the number of stopbands also obeys the periodicity-stopbands number relation showed in Section 2.1. MP structures have more abundant radiation modes, simultaneously dualistic radiations and multi-beam properties. For instance, DP structure simultaneously has one right-handed (parallel phase and group velocities) and one left-handed (antiparallel phase and group velocities) radiation modes in the leaky-wave region at 6.5 GHz. Since two values of β are different, based on the leaky-wave theory, it also has two separated radiation beams. Similarly, for the TP case, it has more right/left-handed radiation modes at a specified frequency. In summary, MP structures can realize multi-beam performance.

For the dispersive (CRLH) TLs, the transmission matrix is [4]

$$\begin{bmatrix} A_m & B_m \\ C_m & D_m \end{bmatrix} = \begin{bmatrix} 1 + Z_m Y_m/2 & Z_m(1 + Z_m Y_m/4) \\ Y_m & 1 + Z_m Y_m/2 \end{bmatrix} \tag{9}$$

where

$$Z_m = j\left(\omega L_{Rm} - \frac{1}{\omega C_{Lm}}\right), \quad Y_m = j\left(\omega C_{Rm} - \frac{1}{\omega L_{Lm}}\right) \tag{10}$$

Here L_{Rm}, L_{Lm}, C_{Rm}, and C_{Lm} are lumped inductances and capacitances, respectively. The equivalent circuit model is same with Figure 1(b). To examine the theory, we simulate Metal-

Insulation-Metal (MIM) CRLH structures in HFSS. Comparisons of theoretical and simulation results are presented in Figures 3(d)–(f). Conclusions are same with those of MP CRLH media. However, through our implementation, MP CRLH TLs' impedance matching is very challenging.

3. MULTIPLE PERIODIC PHASE REVERSAL ANTENNA

In this part, MP PR antennas are proposed. PR antenna is a periodically loaded antenna. It is introduced in [5]. The PR UC is presented in Figure 4(a). To realize the MP configuration, different UCs are set up by changing the characteristic impedances. Figure 4(b) shows the prototypes of SP, DP and TP PR antennas. We varied the dimensions of W from 30 to 70 mil (step is 20 mil) for SP, DP and TP cases. The PR antenna is a TEM type TL. We can characterize the dispersion relation

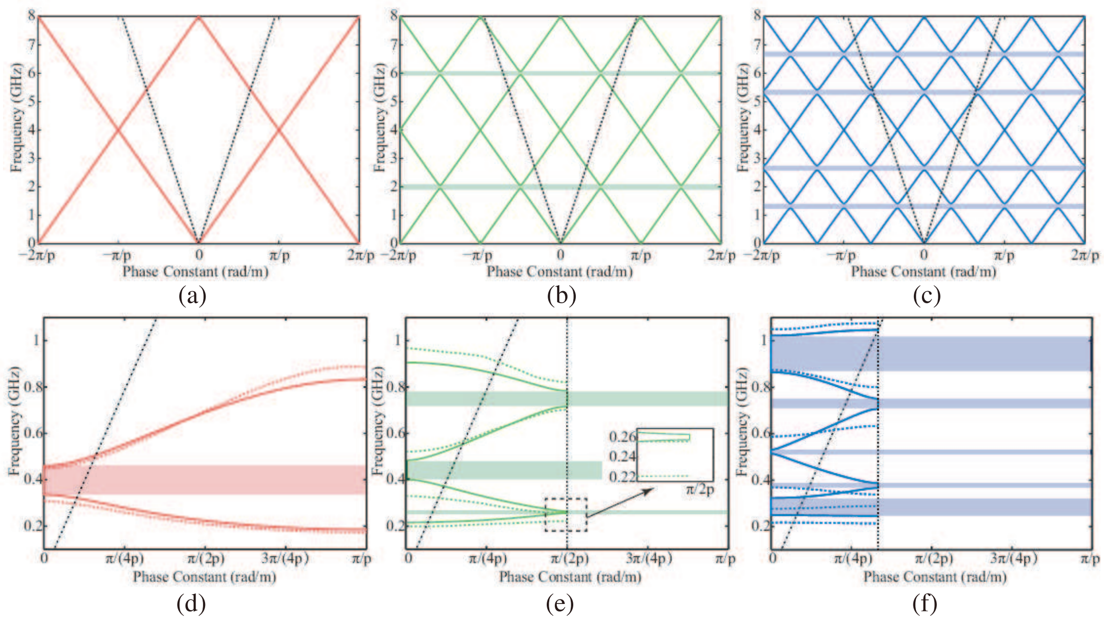

Figure 3: Dispersion relations for (a)–(c) non-dispersive and (d)–(f) dispersive SP, DP and TP circuits. The solid lines are the dispersion curves. The black and colored dash lines are the wave vectors in the free space (air lines) and full wave simulated CRLH dispersion curves. The shadow regions refer to stopbands.

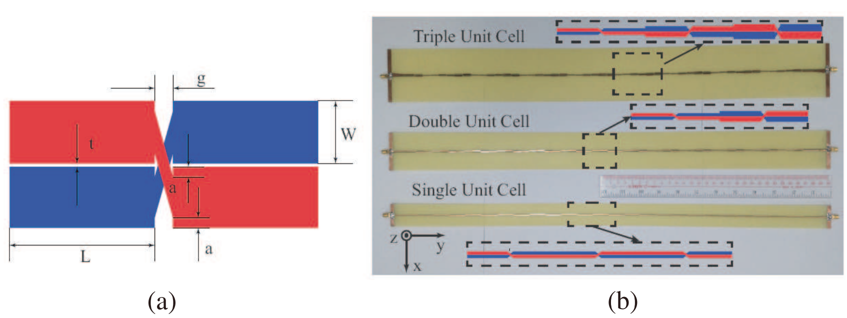

Figure 4: (a) UC of PR antenna and (b) prototypes of SP, DP and TP PR antennas.

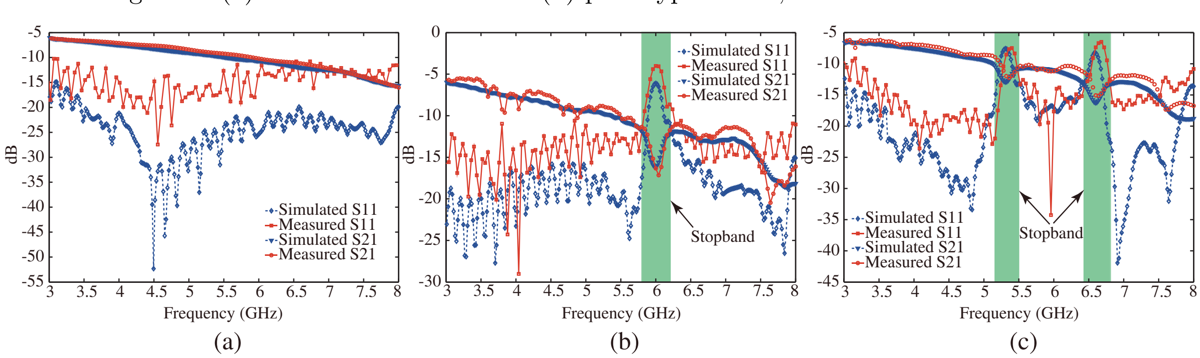

Figure 5: Simulated and measured S-parameters of (a) SP, (b) DP and (c) TP PR antennas.

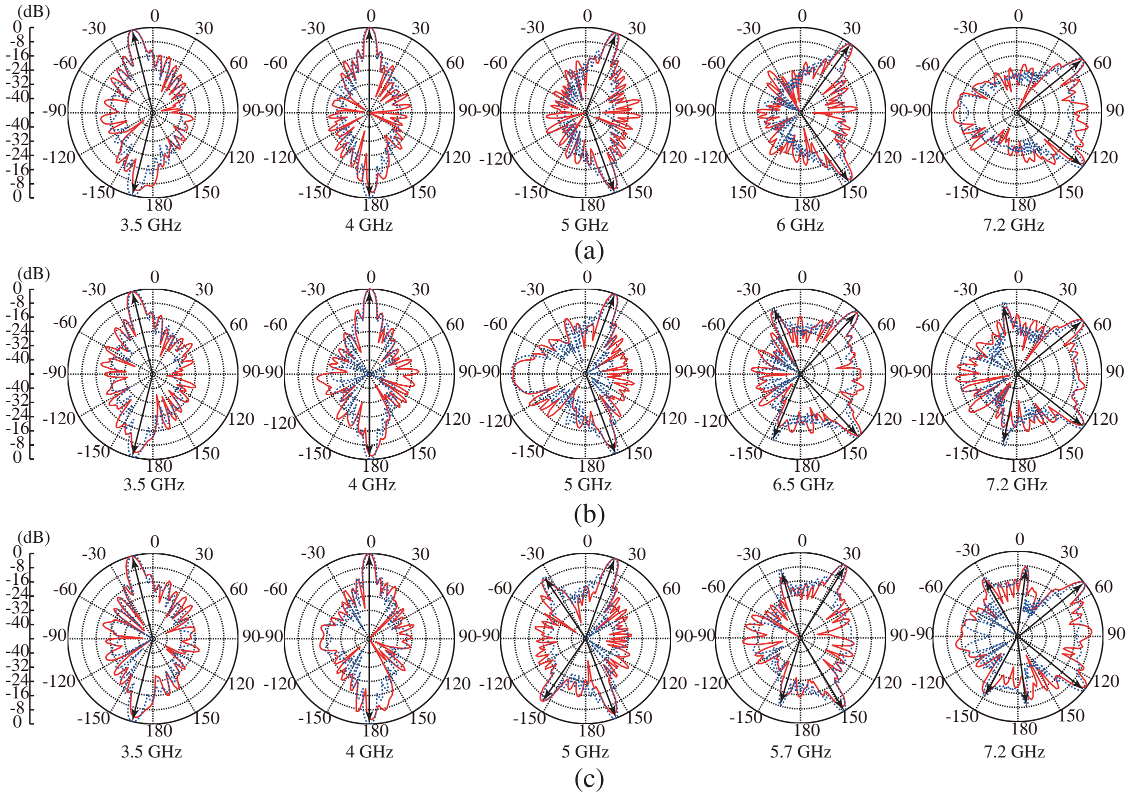

Figure 6: Simulated (red lines) and measured (blue lines) radiation patterns in y-z plane for (a) SP, (b) DP and (c) TP PR antennas.

of PR antennas based on the strip line TL model. But there is a difference, an extra frequency-independent π phase shift is generated per UC due to phase reversal. The dispersion relations of SP, DP, TP PR antennas can be obtained by simply shifting each space harmonic modes with π rad in dispersion diagrams of strip lines, as shown in Figures 3(a)–(c). Figures 5(d)–(f) present the simulated and measured S-parameters of SP, DP and TP PR antennas. Figure 6 shows the normalized simulated and measured radiation patterns of three antennas in y-z plane. It is very obvious that DP antenna at $\{6.5, 7.2\}$ GHz and TP antenna at $\{5, 5.7\}$ GHz all have two radiation modes. At these frequencies, both right- and left-handed radiations are excited. These beams scan with the frequency change. At 7.2 GHz, TP antenna has three radiation modes, and three beams are generated in each half plane. The radiation patterns show very good agreements with dispersion relations.

4. CONCLUSION

The dispersion relations of the general MP structure are analyzed theoretically for layered media and lumped circuits. Both non-dispersive and dispersive materials are discussed for each case. A unified dispersion relation formula and a general Bragg condition are presented. The transmission and radiation performances of MP structures are examined by MP PR antennas. The measurement results present very good agreements with the theories.

REFERENCES

1. Saleh, B. E. A. and M. C. Teich, *Fundamentals of Photonics*, 2nd Edition, Wiley, New York, 2007.
2. Ishimaru, A., *Electromagenetic Wave Propagation, Radiation, and Scattering*, Prentice-Hall, 1991.
3. Oliner, A. A. and D. R. Jackson, "Leaky-wave antennas," *Antenna Engineering Handbook*, 4th Edition, Ch. 10, J. Volakis, Ed., McGraw-Hill, New York, 2007.
4. Caloz, C. and T. Itoh, *Electromagnetic Metamaterials: Transmission Line Theory and Microwave Applications*, Wiley, New York, 2006.
5. Yang, N., C. Caloz, and K. Wu, "Full-space scanning periodic phase-reversal leaky-wave antenna," *IEEE Trans. Antennas Popag.*, Vol. 58, No. 10, 2619–2632, Oct. 2010.